Constraint Singularity-Free Design of the IRSBot-2

Coralie Germain, Sébastien Briot, Stéphane Caro, Philippe Wenger

▶ **To cite this version:**

Coralie Germain, Sébastien Briot, Stéphane Caro, Philippe Wenger. Constraint Singularity-Free Design of the IRSBot-2. Advances in Robot Kinematics, Jun 2012, Innsbruck, Austria. hal-00676851

HAL Id: hal-00676851
https://hal.science/hal-00676851

Submitted on 3 Feb 2019

HAL is a multi-disciplinary open access archive for the deposit and dissemination of scientific research documents, whether they are published or not. The documents may come from teaching and research institutions in France or abroad, or from public or private research centers.

L'archive ouverte pluridisciplinaire **HAL**, est destinée au dépôt et à la diffusion de documents scientifiques de niveau recherche, publiés ou non, émanant des établissements d'enseignement et de recherche français ou étrangers, des laboratoires publics ou privés.

Constraint Singularity-Free Design of the IRSBot-2

Coralie Germain, Sébastien Briot, Stéphane Caro and Philippe Wenger

Abstract This paper deals with the constraint analysis of a novel two-degree-of-freedom (DOF) spatial translational parallel robot for high-speed applications named the IRSBot-2 (acronym for IRCCyN Spatial Robot with 2 DOF). Unlike most two-DOF robots dedicated to planar translational motions this robot has two spatial kinematic chains that provide a very good intrinsic stiffness. First, the robot architecture is presented and its constraint singularity conditions are given. Then, its constraint singularities are analyzed in its parameter space based on a cylindrical algebraic decomposition. Finally, a deep analysis is carried out in order to determine the sets of design parameters of the IRSBot-2 that prevent it from reaching any constraint singularity. To the best of our knowledge, such an analysis is performed for the first time.

Key words: parallel manipulator, constraint singularity, cylindrical algebraic decomposition, design.

1 Introduction

Several robot architectures with two translational degrees of freedom (DOF) for high-speed operations have been proposed in the past decades. Brogårdh proposed in [2] an architecture made of a parallelogram joint (also called Π joint) located between the linear actuators and the platform. Another two-DOF translational robot was presented in [5], where the authors use two Π joints to link the platform with two vertical prismatic actuators. Its equivalent architecture actuated by revolute joints is presented in [4].

Coralie Germain, Sébastien Briot, Stéphane Caro, Philippe Wenger
Institut de Recherche en Communications et Cybernétique de Nantes, France e-mail: {germain,briot,caro,wenger}@irccyn.ec-nantes.fr

The foregoing architectures are all planar, i.e., their elements are constrained to move in the plane of motion. As a result, their elements are all subject to bending effects in the direction normal to the plane of motion. In order to guarantee a minimum stiffness in this direction, the elements have to be bulky, leading to high inertia and low acceleration capacities. In order to overcome these problems, a new Delta-like robot, named the Par2, was proposed in [7]. However, even if its acceleration capacities are impressive, its accuracy is poor.

A two-DOF spatial translational robot, named IRSBot-2, was introduced in [3] to overcome its counterparts in terms of mass in motion, stiffness and workspace size. The IRSBot-2 has a spatial architecture and the distal parts of its legs are subject only to traction/compression/torsion. As a result, its stiffness is increased and its total mass can be reduced. Nevertheless, the IRSBot-2 may reach some constraint singularities [1, 8]. In this paper, a deep analysis is carried out in order to determine the sets of design parameters of the IRSBot-2 that prevent it from reaching any constraint singularity.

This paper is organized as follows. First, the robot architecture is described and its constraint singularity conditions are given. Then, its constraint singularities are analyzed in its parameter space based on a cylindrical algebraic decomposition. Finally, the set of design parameters for the robot to be free of constraint singularity are determined.

2 Robot Architecture and Constraint Singularity Conditions

The IRSBot-2 is shown in Fig. 1 and is composed of two identical legs linking the fixed base to the moving platform. Each leg contains a proximal module and a distal module, which are illustrated in Fig. 2.

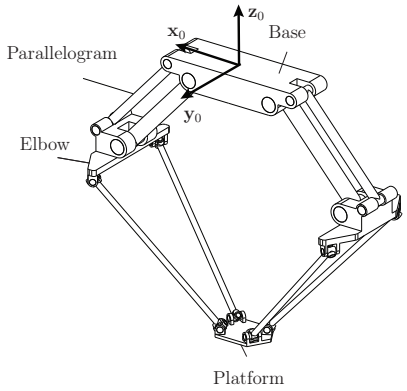

Fig. 1 CAD Modeling of the IRSBot-2

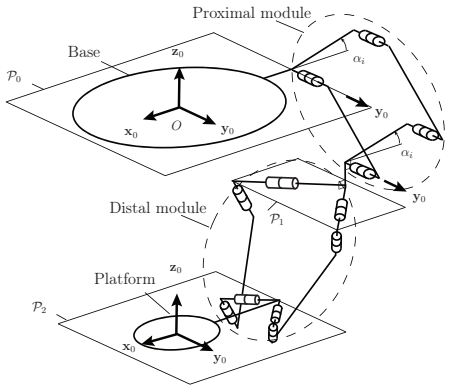

Fig. 2 Kinematic chain of the ith leg ($i = 1, 2$)

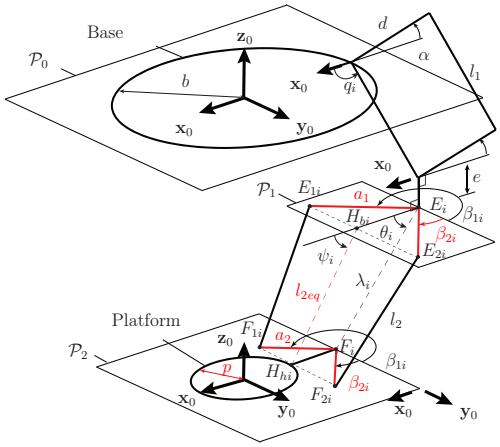

Fig. 3 Paramaterization of the ith leg ($i = 1, 2$)

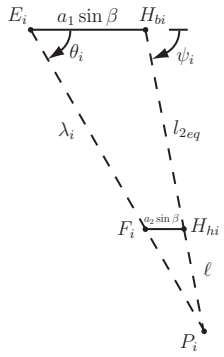

Fig. 4 Closed-loop E_i–H_{bi}–H_{hi}–F_i: projection of the distal module on the plane ($\mathbf{x}_0 O \mathbf{z}_0$)

The parameters of the IRSBot-2 used throughout this paper are depicted in Figs. 3 and 4. From [3], the IRSBot-2 reaches a constraint singularity iff[1]:

$$\theta_1 = \theta_2 + k\pi, \quad k = 0, 1 \tag{1}$$

and

$$(x_{P_2} - x_{P_1}) \cos^2\beta \cos\theta_2 - (z_{P_2} - z_{P_1}) \sin\theta_2 = 0 \tag{2}$$

It is noteworthy that Eqs. (1) and (2) depend only on the design parameters associated with the distal module. Therefore, the proximal modules of the IRSBot-2 do not affect its constraint singularities and we focus only on the constraint singularities associated with the distal modules.

3 Constraint Singularity Analysis of the IRSBot-2 in its Parameter Space

This section aims to find the sets of design parameters (a_1, a_2, β, p, l_{2eq}) that allow the IRSBot-2 to reach some constraint singularities. Note that the foregoing five design parameters are shown in Fig. 3. a_1, a_2 and l_{2eq} are the lengths of segments E_iE_{1i}, F_iF_{1i} and $H_{bi}H_{hi}$, respectively. p is the moving-platform radius. The coordinates of vector $\overrightarrow{P_1P_2}$ can be expressed as:

$$x_{P_2} - x_{P_1} = 2p + \ell(\cos\psi_2 - \cos\psi_1) \tag{3}$$

$$z_{P_2} - z_{P_1} = \ell(\sin\psi_2 - \sin\psi_1) \tag{4}$$

$$\ell = \frac{a_2 l_{2eq}}{a_1 - a_2} \tag{5}$$

[1] Let β denote β_{22}, then $\beta_{11} = \pi + \beta$, $\beta_{21} = -\beta$ and $\beta_{12} = \pi - \beta$

Angles ψ_1 and ψ_2 are depicted in Figs. 3 and 4. From the closed-loop E_i–H_{bi}–H_{hi}–F_i ($i = 1,2$) and Fig. 4, the following relations between λ_i, θ_i and ψ_i are obtained:

$$l_{2eq}\cos\psi_i = \lambda_i\cos\theta_i - (a_1 - a_2)\sin\beta \tag{6}$$

$$-l_{2eq}\sin\psi_i = -\lambda_i\sin\theta_i \tag{7}$$

λ_i is depicted in Fig. 4 and is derived from Eqs. (3) to (7):

$$\lambda_i = \sqrt{l_{2eq}^2 + (a_1 - a_2)^2\sin^2\beta + 2(-1)^{i+1}l_{2eq}\cos\psi_i(a_1 - a_2)\sin\beta} \tag{8}$$

The following three cases, obtained from Eqs. (1) and (8), allow us to simplify Eqs. (3) to (7) to end up with a univariate polynomial form of constraint singularity condition (2):

Case I: $\theta_1 = \theta_2 + \pi$ and $\lambda_1 = \lambda_2 \neq 0$
Case II: $\theta_1 = \theta_2 + \pi$ and $\lambda_1 \neq \lambda_2$
Case III: $\theta_1 = \theta_2$

For Case I, Eq. (2) takes the form:

$$P_I(X) = A_1X^2 + B_1X + C_1 = 0 \tag{9}$$

with

$$\begin{cases} A_1 &= -\,l_{2eq}^2\sin^2\beta\; a_2/(a_1 - a_2) \\ B_1 &= l_{2eq}\,(1 - \sin^2\beta)\,(p - a_2\,\sin\beta) \\ C_1 &= -\,p\,(a_1 - a_2)\,(1 - \sin^2\beta)\,\sin\beta + l_{2eq}^2\,a_2/(a_1 - a_2) \\ & X = \cos\psi,\ \psi = \psi_2,\ X \in [-1,\,1],\ [a_1,\,a_2,\,\beta,\,p] \in \mathscr{D}, \\ & l_{2eq} \in]0,\,+\infty[\end{cases}$$

$\mathscr{D} =]0,\,+\infty[\times]0,\,a_1[\times[0,\,\pi/2]\times]0,\,+\infty[$.

For Case II, Eq. (2) takes the form:

$$P_{II}(X) = A_2X^2 + C_2 = 0 \tag{10}$$

with

$$\begin{cases} A_2 &= a_2\sin^3\beta \\ C_2 &= p(1 - \sin^2\beta) - a_2\sin^3\beta \\ & X = \cos\theta,\ \theta = \theta_2,\ X \in [-1,\,0],\ [a_1,\,a_2,\,\beta,\,p] \in \mathscr{D}, \\ & l_{2eq} \in](a_1 - a_2)\sin\beta|\sin\theta|,\,(a_1 - a_2)\sin\beta[\end{cases}$$

For Case III, Eq. (2) takes the form:

$$P_{III}(X) = A_3X^2 + C_3 = 0 \tag{11}$$

with

$$\begin{cases} A_3 & = a_2 \sin^3\beta \\ C_3 & = p(1-\sin^2\beta) - a_2\sin^3\beta \\ & X = \cos\theta,\ \theta = \theta_2, X \in [-1,1], [a_1, a_2, \beta, p] \in \mathscr{D}, \\ & l_{2eq} \in](a_1 - a_2)\sin\beta, +\infty[\end{cases}$$

As a matter of fact, the IRSBot-2 reaches a constraint singularity as long as one of the univariate polynomials (9), (10), (11) admits one solution at least. The set of design parameters (a_1, a_2, β, p, l_{2eq}) for which the constraint singularities associated with Cases I, II and III can be reached are obtained with a method based on the notion of Discriminant Varieties and Cylindrical Algebraic Decomposition. This method resorts to Gröbner bases for the solutions of systems of equations and is described in [6]. Besides, the tools used to perform the computations are implemented in a Maple library called Siropa[2].

Table 1 Formulae describing the boundaries of the cells in Tables 2, 3 and 4

$a_{11} = 0$	$p_1 = 0$
$a_{12} = +\infty$	$p_2(a_1,a_2,\beta) = \frac{1-\sin\beta}{1+\sin\beta} a_2 \sin\beta$
$a_{21} = a_1$	$p_3(a_1,a_2,\beta) = \frac{1-\sin^2\beta}{1+\sin^2\beta} a_2 \sin\beta$
$a_{22} = +\infty$	$p_4(a_1,a_2,\beta) = a_2 \sin\beta$
$\beta_1 = 0$	$p_5(a_1,a_2,\beta) = \frac{1+\sin^2\beta}{1-\sin^2\beta} a_2 \sin\beta$
$\beta_2 = \arcsin(1/\sqrt{3})$	$p_6(a_1,a_2,\beta) = \frac{1+\sin\beta}{1-\sin\beta} a_2 \sin\beta$
$\beta_3 = \pi/4$	$p_7 = +\infty$
$\beta_4 = \pi/2$	$p_8(a_1,a_2,\beta) = a_2 \sin\beta \tan^2\beta$
$l_{2eq_1}(a_1,a_2,\beta,p) = \frac{a_1-a_2}{a_2}\ p$	
$l_{2eq_2}(a_1,a_2,\beta,p) = (a_1-a_2)\ \sin\beta$	
$l_{2eq_3}(a_1,a_2,\beta,p) = \frac{a_1-a_2}{2a_2\sin\beta} \sqrt{(\sin^2\beta-1)\left[(\sin^2\beta-1)(p-a_2\sin\beta)^2 + 4\,p\,a_2\sin^3\beta\right]}$	
$l_{2eq_4}(a_1,a_2,\beta,p) = (a_1-a_2)\ \sin\beta\lvert\sin\theta\rvert$	
$l_{2eq_4}(a_1,a_2,\beta,p) = +\infty$	

Table 1 provides the different formulae bounding the five-dimensional cells associated with Cases I, II and III. a_1 and β can be chosen independently. Then, the boundaries for a_2, p are l_{2eq} are determined successively. Table 2 characterizes all the cells where the IRSBot-2 can reach a constraint singularity, namely, where P_I, P_{II} or P_{III} has at least one real root. It is noteworthy that a real root of one the three foregoing polynomials amounts to two symmetrical singular configurations of the distal module. It is apparent that six cells arise where P_I has a single real root, two cells arise where P_I has two real roots. P_{II} and P_{III} can get two real roots in one cell only. Some constraint singularities of the IRSBot-2 are shown in [3].

[2] http://www.irccyn.ec-nantes.fr/~chablat/SIROPA/files/siropa-mpl.html

[3] http://www.irccyn.ec-nantes.fr/IRSBot2

Table 2 Cells of $\mathbb{R}^5$ where the IRSBot-2 can reach constraint singularities

Case I			
$(]a_{11},a_{12}[,]a_{21},a_{22}[,]\beta_1,\beta_4[)$	$]p_1,p_2[$	$(]l_{2eq_1},l_{2eq_2}[)$	Two singular configs.
	$]p_2,p_3[$	$(]l_{2eq_1},l_{2eq_2}[)$	
	$]p_3,p_4[$	$(]l_{2eq_1},l_{2eq_2}[)$	
	$]p_4,p_5[$	$(]l_{2eq_2},l_{2eq_1}[)$	
	$]p_5,p_6[$	$(]l_{2eq_2},l_{2eq_1}[)$	
	$]p_6,p_7[$	$(]l_{2eq_2},l_{2eq_1}[)$	
	$]p_3,p_4[$	$(]l_{2eq_3},l_{2eq_1}[)$	Four singular configs.
	$]p_4,p_5[$	$(]l_{2eq_3},l_{2eq_2}[)$	
Case II			
$(]a_{11},a_{12}[,]a_{21},a_{22}[,]\beta_1,\beta_4[)$	$]p_1,p_8[$	$(]l_{2eq_4},l_{2eq_2}[)$	Four singular configs.
Case III			
$(]a_{11},a_{12}[,]a_{21},a_{22}[,]\beta_1,\beta_4[)$	$]p_1,p_8[$	$(]l_{2eq_1},l_{2eq_2}[)$	Four singular configs.

4 Design Parameters for the IRSBot-2 to be Free of Constraint Singularity

This section aims to find the sets of design parameters (a_1, a_2, β, p, l_{2eq}) that prevent the IRSBot-2 from reaching any constraint singularity. It amounts to find the intersection of cells where P_I, P_{II} and P_{III} do not have any real root over their mutual domain.

It turns to be quite difficult to obtain the intersection of cells contrary to their union. As a consequence, we will search for the cells where the product of P_I, P_{II} and P_{III} does not have any real root. From (10) and (11), it is apparent that the expressions of P_{II} and P_{III} are the same, but their domains are disjointed and complementary because of the bounds of l_{2eq}. Therefore, the sets of design parameters (a_1, a_2, β, p, l_{2eq}) that prevent the IRSBot-2 from reaching any constraint singularity correspond to the union of cells that do not provide any real root for the following two univariate polynomials:

$$P_{IV}(X) = P_I P_{II}(X) = (A_1X^2 + B_1X + C_1)(A_2((X-1)/2)^2 + C_2) = 0 \tag{12}$$

with

$$\begin{cases} X \in [-1,1], [a_1, a_2, \beta, p] \in \mathscr{D}, \\ l_{2eq} \in]|\sin\theta|(a_1 - a_2)\ \sin\beta, (a_1 - a_2)\sin\beta[\end{cases}$$

and

$$P_V(X) = P_I P_{III}(X) = (A_1X^2 + B_1X + C_1)(A_3X^2 + C_3) = 0 \tag{13}$$

with

$$\begin{cases} X \in [-1,1], [a_1, a_2, \beta, p] \in \mathscr{D}, \\ l_{2eq} \in](a_1 - a_2)\sin\beta, +\infty[\end{cases}$$

A_1, B_1, C_1, A_2, C_2, A_3, C_3 and $\mathscr{D}$ being defined in Eqs. (9) to (11).

Eq. (12) amounts to the product of P_I and P_{II} with a change a variable for P_{II} and the most restrictive domain for l_{2eq} defined in (10), whereas Eq. (13) amounts to the product of P_I and P_{III} with the most restrictive domain for l_{2eq} defined in (11). Table 1 gives the different formulae bounding the five-dimensional cells associated with (12) and (13). The cells where P_{IV} and P_V do not have any real root, i.e., the sets of design parameters $(a_1, a_2, \beta, p, l_{2eq})$ that prevent the IRSBot-2 from reaching any constraint singularity, are expressed in Tables 3 and 4, respectively.

Table 3 Cells where Eq. (12) does not have any real root with $a_1 \in]a_{11}, a_{12}[$ and $a_2 \in]a_{21}, a_{22}[$

$[\beta_1, \beta_2[$	$(]p_8, p_3[,]l_{2eq4}, l_{2eq1}[)$, $(]p_3, p_4[,]l_{2eq4}, l_{2eq3}[)$, $(]p_4, p_5[,]l_{2eq4}, l_{2eq3}[)$, $(]p_5, p_7[,]l_{2eq4}, l_{2eq2}[)$
$[\beta_2, \beta_3[$	$(]p_8, p_4[,]l_{2eq4}, l_{2eq3}[)$, $(]p_4, p_5[,]l_{2eq4}, l_{2eq3}[)$, $(]p_5, p_7[,]l_{2eq4}, l_{2eq2}[)$
$[\beta_3, \beta_4]$	$(]p_8, p_5[,]l_{2eq4}, l_{2eq3}[)$, $(]p_5, p_7[,]l_{2eq4}, l_{2eq2}[)$

Table 4 Cells where Eq. (13) does not have any real root with $a_1 \in]a_{11}, a_{12}[$ and $a_2 \in]a_{21}, a_{22}[$

$[\beta_1, \beta_2[$	$(]p_8, p_3[,]l_{2eq2}, l_{2eq5}[)$, $(]p_3, p_4[,]l_{2eq2}, l_{2eq5}[)$, $(]p_4, p_5[,]l_{2eq1}, l_{2eq5}[)$, $(]p_5, p_7[,]l_{2eq1}, l_{2eq5}[)$
$[\beta_2, \beta_3[$	$(]p_8, p_4[,]l_{2eq2}, l_{2eq5}[)$, $(]p_4, p_5[,]l_{2eq1}, l_{2eq5}[)$, $(]p_5, p_7[,]l_{2eq1}, l_{2eq5}[)$
$[\beta_3, \beta_4]$	$(]p_8, p_5[,]l_{2eq1}, l_{2eq5}[)$, $(]p_5, p_7[,]l_{2eq1}, l_{2eq5}[)$

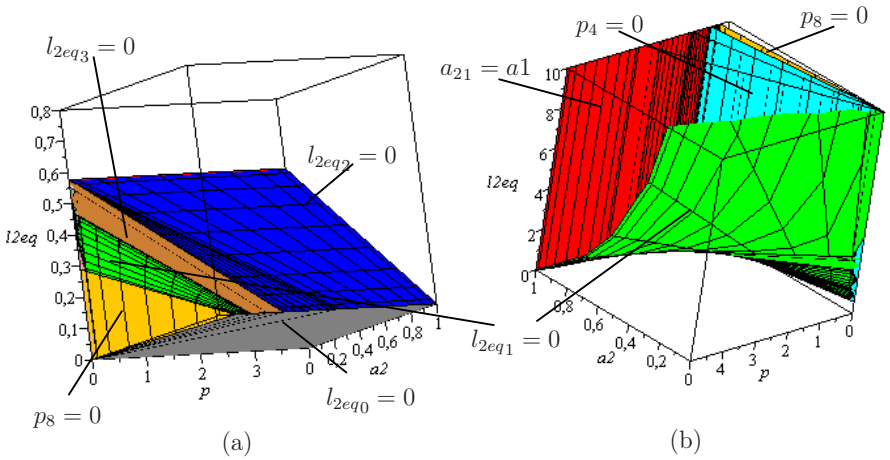

Fig. 5 Cells where the IRSBot-2 cannot reach any constraint singularity for: (a) $a_1 = 1, \beta = \arcsin(1/\sqrt{3})$ and $l_{2eq} < (a_1 - a_2)\sin\beta$; (b) $a_1 = 1, \beta = \arcsin(1/\sqrt{3})$ and $l_{2eq} > (a_1 - a_2)\sin\beta$

Figure 5(a) (Fig. 5(b), resp.) illustrates the cells where Eq. (12) (Eq. (13), resp.) does not have any real root, namely, the sets of design parameters that prevent the IRSBot-2 from reaching any constraint singularity for $a_1 = 1, \beta = \arcsin(1/\sqrt{3})$ and $l_{2eq} < (a_1 - a_2)\sin\beta$ ($l_{2eq} > (a_1 - a_2)\sin\beta$, resp.). We can notice that the amount

of constraint singularity-free designs is higher with $l_{2eq} > (a_1 - a_2)\sin\beta$ than with $l_{2eq} < (a_1 - a_2)\sin\beta$.

5 Conclusions

This paper dealt with the constraint analysis of the IRSBot-2 throughout its parameter space. Its constraint singularities were analyzed in its parameter space with a method based on the notion of Discriminant Varieties and Cylindrical Algebraic Decomposition. This method allowed us to convert a kinematic problem into an algebraic one. Then, a deep analysis was carried out in order to determine the sets of design parameters of the distal modules that prevent the IRSBot-2 from reaching any constraint singularity. To the best of our knowledge, such an analysis had never been performed before. The design parameters associated with the proximal modules for the IRSBot-2 to be assembled will be determined in a future work.

6 Acknowledgment

This work was conducted with the support of the French National Research Agency (Project ANR-2011-BS3-006-01-ARROW). The authors also thank Damien Chablat for his great help with the Siropa Maple library.

References

1. Amine, S., Tale-Masouleh, M., Caro, S., Wenger, P., Gosselin, C.: Singularity Conditions of 3T1R Parallel Manipulators with Identical Limb Structures. ASME Journal of Mechanisms and Robotics (2012). DOI 10.1115/1.4005336
2. Brogardh, T.: Device for relative movement of two elements. Patent US 6301988 B1 (2001)
3. Germain, C., Briot, S., Glazunov, V., Caro, S., Wenger, P.: Irsbot-2: A novel two-dof parallel robot for high-speed operations. In: Proceedings of the ASME 2011 International Design Engineering Technical Conferences & Computers and Information in Engineering Conference. Washington, DC, USA, August, 29-31 (2011)
4. Huang, T., Li, M., Li, Z., Chetwynd, D., Whitehouse, D.: Planar parallel robot mechanism with two translational degrees of freedom. Patent WO 03055653 A1 (2003)
5. Liu, X., Kim, J.: Two novel parallel mechanisms with less than six degrees of freedom and the applications. In: Proc. Workshop on Fundamental Issues and Future Reserch Directions for Parallel Mechanisms and Manipulators, pp. 172–177. Quebec city, Quebec, Canada (2002)
6. Moroz, G., Chablat, D., Wenger, P., Rouiller, F.: Cusp points in the parameter space of rpr-2prr parallel manipulator. In: 3-rd European Conference on Mechanism Science, Cluj-Napoca, Romania, Springer, pp. 29–37 (2010)
7. Pierrot, F., Krut, S., Company, O., Nabat, V., Baradat, C., Fernandez, A.S.: Two degree-of-freedom parallel manipulator. Patent WO 2009/089916 A1 (2009)
8. Zlatanov, D., Bonev, I., Gosselin, C.: Constraint singularities of parallel mechanisms. In: Proc. 2002 IEEE International Conference on Robotics and Automation, pp. 496–502 (2002)